TELKOMNIKA Telecommunication, Computing, Electronics and Control
Vol. 24, No. 1, February 2026, pp. 14∼21
ISSN: 1693-6930, DOI: 10.12928/TELKOMNIKA.v24i1.26892

Secure hybrid power-frequency multiple access in satellite terrestrial communication systems: a performance study

Huu Q. Tran and Viet-Thanh Pham
Department of Electronics and Telecommunication, Faculty of Electronics Technology, Industrial University of Ho Chi Minh City, Ho Chi Minh City, Vietnam

Article Info

Article history:

Received Jan 3, 2025
Revised Oct 29, 2025
Accepted Dec 8, 2025

Keywords:

Hybrid power-frequency multiple access
Intercept probability
Outage probability
Satellite-terrestrial systems
Shadowed-Rician fading

ABSTRACT

This paper investigates a secure hybrid power–frequency multiple access (PFMA) framework for satellite–terrestrial communications. By integrating power- and frequency-domain multiplexing, PFMA achieves approximately 4 dB lower transmit signal-to-noise ratio (SNR) than non-orthogonal multiple access (NOMA) for the same connection outage probability (COP) at SNR $>$ 0 dB, and it reduces the COP by up to 30% at low-to-medium SNRs. It further decreases the intercept probability (IP) by 20–25% at $P_S = 10$ dBm. Closed-form COP and IP expressions are derived under shadowed-Rician fading with both internal and external eavesdroppers and validated via Monte Carlo simulations. Parameter analysis indicates that PFMA's SNR gain can either extend coverage by 60% or save 37% energy, providing design guidelines for 6G, satellite IoT, and emergency communication systems. The single-cell assumption points to future work on multi-cell and mobility scenarios.

Corresponding Author:

Huu Q. Tran
Department of Electronics and Telecommunication, Faculty of Electronics Technology
Industrial University of Ho Chi Minh City
Go Vap District, Ho Chi Minh City, Vietnam
Email: tranquyhuu@iuh.edu.vn

1. INTRODUCTION

Satellite–terrestrial communication systems are a foundation for next-generation networks, enabling reliable and ubiquitous connectivity. Among multiple access techniques, hybrid power–frequency multiple access (HPFMA) combines power- and frequency-domain multiplexing to enhance spectral efficiency. However, its security and performance can be hindered by shared channels and the complexities of hybrid architectures [1], [2]. Existing studies have explored improvements via relay protocols, energy harvesting, intelligent reflecting surfaces (IRS), and spectrum sharing [3]-[10]. Secure HPFMA performance under realistic fading and dual eavesdropping scenarios is still underexplored. This work fills that gap via a comprehensive performance analysis of secure HPFMA in satellite–terrestrial systems, focusing on reliability–security trade-offs and design insights for 6G and satellite IoT.

Table 1 contrasts our work with prior studies. Unlike [11]-[13], which focus on non-orthogonal multiple access (NOMA) or simplified fading, we derive closed-form connection outage probability (COP) and intercept probability (IP) for power-factor multiple access (PFMA) under shadowed-Rician fading with both internal and external eavesdroppers. Contributions: (i) closed-form COP, IP, their asymptotics, and diversity order for PFMA under shadowed–Rician fading with both internal and external eavesdroppers; PFMA requires

≈4 dB lower SNR than NOMA for the same COP at SNR > 0 dB; (ii) Monte Carlo validation across diverse parameters, showing superior COP over NOMA at low-to-medium signal-to-noise ratio (SNR); and (iii) parameter study (power, antennas, shadowed–Rician parameters, bandwidth) revealing up to 60% coverage gain or 37% energy saving.

Table 1. Comparison with related works

Ref.	Model	Metrics	Channel	Eavesdropping	Limitations	Our contribution
[3]	NOMA	Secrecy rate	Rayleigh	External	No closed-form COP/IP	Closed-form COP and IP for PFMA
[4]	NOMA	Outage, ergodic capacity (EC)	Nakagami-m	None	Simplified fading	Shadowed–Rician, dual eavesdroppers
[13]	NOMA	COP	Rician	Internal	No external case	Dual eavesdroppers with PFMA
[14]	Partial-NOMA	Secrecy rate	Rayleigh	Internal	No frequency-domain analysis	Hybrid power–frequency, closed-form metrics
[15]	NOMA	IP	Rayleigh	Internal	Simplified channel	Shadowed–Rician with asymptotics
Ours	PFMA	COP, IP, diversity order (DO)	Shadowed–Rician	Internal and external	–	First closed-form COP/IP for PFMA; ∼4 dB SNR gain over NOMA

2. SYSTEM MODEL

Consider Figure 1, where a satellite (S) employs three subcarriers ($s_{\rm B}$, $s_{\rm R}$, $s_{\rm RB}$) to transmit the confidential signal $x_{\rm R}$ to Roy (R) and the secure signal $x_{\rm B}$ to Bob (B). Subcarriers $s_{\rm B}$ and $s_{\rm R}$ occupy bandwidth portions (BPs) $\alpha_{\rm B}$ and $\alpha_{\rm R}$, respectively, and carry $x_{\rm B}$ and $x_{\rm R}$ using orthogonal multiple access (OMA). Meanwhile, a superposition signal $x_{\rm RB} = \sqrt{\beta_{\rm R}}\, x_{\rm R} + \sqrt{\beta_{\rm B}}\, x_{\rm B}$ with power-allocation (PA) factors $\beta_{\rm R}, \beta_{\rm B}$ corresponds to NOMA on $s_{\rm RB}$ with BP $\alpha_{\rm RB}$. Bob and Roy combine their received signals after baseband recovery without successive interference cancellation (SIC). The BP/PA rules are $\alpha_{\rm R} + \alpha_{\rm B} + \alpha_{\rm RB} = 1$, $\beta_{\rm B} + \beta_{\rm R} = 1$, and $\alpha_{\rm RB} \le \alpha_{\rm B}, \alpha_{\rm R}$. Here, α_Q ($Q \in \{B, R\}$) denotes the OMA BPs, while $\alpha_{\rm RB}$ is the PFMA superposition BP; $\beta_{\rm B}$ and $\beta_{\rm R}$ are NOMA PA factors. Unless stated otherwise, receivers are assumed to have perfect SIC when required by a scheme definition.

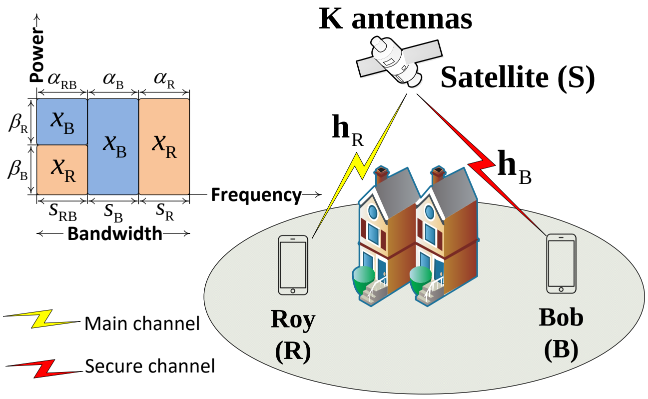

Figure 1. System model of hybrid PFMA in satellite–terrestrial communication

2.1. Propagation and beamforming

Roy acts as an internal eavesdropper and may use SIC to recover Bob's message. All channels $\mathbf{h}_{\rm Q}$ are quasi-static shadowed–Rician with ${\rm Q} \in \{{\rm R}, {\rm B}\}$. channel estimation errors (CEEs) render perfect channel state information (CSI) difficult; CSI is estimated via minimum mean square error (MMSE). The effective channel is:

$$\mathbf{h}_{\rm Q} = \mathbf{g}_{\rm Q}^{\dagger}\mathbf{w}_{\rm Q}\sqrt{L_{\rm SQ}\,\vartheta_S\,\vartheta(\theta_{\rm Q})} \tag{1}$$

Here, $\mathbf{g}_\mathrm{Q} \in \mathbb{C}^{K\times 1}$ is the shadowed–Rician vector (S→Q), $\mathbf{w}_\mathrm{Q} \in \mathbb{C}^{K\times 1}$ is maximum ratio transmission (MRT):

$$\mathbf{w}_\mathrm{Q} = \frac{\mathbf{g}_\mathrm{Q}}{\|\mathbf{g}_\mathrm{Q}\|_F} \tag{2}$$

The free-space loss is:

$$L_\mathrm{SQ} = \frac{1}{\mathcal{K}_B T W}\left(\frac{c}{4\pi f_c d_\mathrm{SQ}}\right)^2 \tag{3}$$

with $\mathcal{K}_B = 1.38 \times 10^{-23}$ J/K, T the noise temperature, W the bandwidth, c the speed of light, f_c the carrier, and d_SQ the S–Q distance [16]. The satellite beam gain is:

$$\vartheta(\theta_\mathrm{Q}) = \vartheta_\mathrm{Q}\left(\frac{I_1(\bar{\rho}_\mathrm{Q})}{2\bar{\rho}_\mathrm{Q}} + 36\,\frac{I_3(\bar{\rho}_\mathrm{Q})}{\bar{\rho}_\mathrm{Q}^3}\right) \tag{4}$$

where $I_i(\cdot)$ is the ith-order Bessel function (first kind), $\bar{\rho}_\mathrm{Q} = 2.07123\,\frac{\sin\theta_\mathrm{Q}}{\sin\theta_{\mathrm{Q},3\mathrm{dB}}}$, and $\theta_{\mathrm{Q},3\mathrm{dB}}$ is the 3 dB beamwidth.

2.2. Signal processing at Q

The received baseband signal at $Q \in \{\mathrm{R}, \mathrm{B}\}$ is:

$$\bar{y}_\mathrm{Q} = \begin{cases} \sqrt{\alpha_\mathrm{Q} P_S L_\mathrm{SQ} \vartheta_S \vartheta(\theta_\mathrm{Q})}\, x_\mathrm{Q}\, \mathbf{g}_\mathrm{Q}^\dagger \mathbf{w}_\mathrm{Q} + n_\mathrm{Q}, & s_\mathrm{Q} \\ \sqrt{\alpha_\mathrm{RB} P_S L_\mathrm{SQ} \vartheta_S \vartheta(\theta_\mathrm{Q})}\, x_\mathrm{RB}\, \mathbf{g}_\mathrm{Q}^\dagger \mathbf{w}_\mathrm{Q} + n_\mathrm{Q}, & s_\mathrm{RB} \end{cases} \tag{5}$$

where P_S is the satellite transmit power and $n_\mathrm{Q} \sim \mathcal{CN}(0, \sigma_\mathrm{Q}^2)$. Define $\nu_\mathrm{Q} = \alpha_\mathrm{Q} + \alpha_\mathrm{RB}\beta_\mathrm{Q}$ and $\mu_\mathrm{Q} = \alpha_\mathrm{Q} + \alpha_\mathrm{RB}$. The aggregate SINR for decoding x_Q at Q is [17].

$$\bar{\gamma}_\mathrm{Q} = \frac{\nu_\mathrm{Q}\,\delta_\mathrm{Q}\,\|\mathbf{g}_\mathrm{Q}\|_F^2}{\nu_\mathrm{Q}\,\delta_\mathrm{Q}\,\|\mathbf{g}_\mathrm{Q}\|_F^2 + \mu_\mathrm{Q}} = \frac{\nu_\mathrm{Q}\,\mathcal{A}_\mathrm{Q}}{\nu_\mathrm{Q}\,\mathcal{A}_\mathrm{Q} + \mu_\mathrm{Q}} \tag{6}$$

where $\varrho_S = P_S/\sigma_\mathrm{Q}^2$ is the SNR, $\mathcal{A}_\mathrm{Q} = \delta_\mathrm{Q}\|\mathbf{g}_\mathrm{Q}\|_F^2$, and $\delta_\mathrm{Q} = \varrho_S L_\mathrm{SQ} \vartheta_S \vartheta(\theta_\mathrm{Q})$. After canceling its own data via SIC, Roy tries to intercept x_B with:

$$\hat{\gamma}_\mathrm{R} = \frac{\alpha_\mathrm{RB}\beta_\mathrm{B}\,\delta_\mathrm{R}\,\|\mathbf{g}_\mathrm{R}\|_F^2}{\mu_\mathrm{R}} = \frac{\nu_\mathrm{R}\,\mathcal{A}_\mathrm{R}}{\mu_\mathrm{R}} \tag{7}$$

2.3. Terrestrial channel model

Assuming i.i.d. coefficients, the probability density function (PDF) of $|g_\mathrm{Q}^{(k)}|^2$ (S→Q, kth antenna) under shadowed–Rician fading is:

$$f_{|g_\mathrm{Q}^{(k)}|^2}(x) = \alpha_\mathrm{Q} e^{-\beta_\mathrm{Q} x}\, {}_1F_1(m_\mathrm{Q}; 1; \varpi_\mathrm{Q} x), \quad x \geq 0 \tag{8}$$

with,

$$\alpha_\mathrm{Q} = \left[\frac{2b_\mathrm{Q} m_\mathrm{Q}}{2b_\mathrm{Q} m_\mathrm{Q} + \Omega_\mathrm{Q}}\right]^{m_\mathrm{Q}} \Big/ (2b_\mathrm{Q}), \quad \beta_\mathrm{Q} = \frac{1}{2b_\mathrm{Q}}, \quad \varpi_\mathrm{Q} = \frac{\Omega_\mathrm{Q}(2b_\mathrm{Q} m_\mathrm{Q} + \Omega_\mathrm{Q})}{2b_\mathrm{Q}}$$

Here, Ω_Q (LOS power), $2b_\mathrm{Q}$ (diffuse power), and m_Q (fading severity) follow [18]. For integer m_Q,

$$f_{|g_\mathrm{Q}^{(k)}|^2}(x) = \alpha_\mathrm{Q} e^{-(\beta_\mathrm{Q} - \varpi_\mathrm{Q})x} \sum_{t=0}^{m_\mathrm{Q}-1} \zeta_\mathrm{Q}(t)\, x^t, \quad \zeta_\mathrm{Q}(t) = \frac{(-1)^t (1 - m_\mathrm{Q})_t \varpi_\mathrm{Q}^t}{(t!)^2} \tag{9}$$

Using Bankey *et al*. [19], the PDF of $\mathcal{A}_\mathrm{Q}$ is:

$$f_{\mathcal{A}_{\mathrm{Q}}}(x) = \sum_{j_1=0}^{m_{\mathrm{Q}}-1} \cdots \sum_{j_K=0}^{m_{\mathrm{Q}}-1} \frac{\Lambda_{\mathrm{Q}}(K)}{\delta_{\mathrm{Q}}^{\Delta_{\mathrm{Q}}}} x^{\Delta_{\mathrm{Q}}-1} \exp\left(-\frac{\psi_{\mathrm{Q}}}{\delta_{\mathrm{Q}}} x\right) \tag{10}$$

where,

$$\Lambda_{\mathrm{Q}}(K) = \alpha_{\mathrm{Q}}^{K} \prod_{l=1}^{K} \zeta_{\mathrm{Q}}(j_l) \prod_{u=1}^{K-1} \mathcal{B}\left(\sum_{p=1}^{u} j_p + u,\, j_{u+1} + 1\right), \Delta_{\mathrm{Q}} = \sum_{l=1}^{K} j_l + K, \quad \psi_{\mathrm{Q}} = \beta_{\mathrm{Q}} - \delta_{\mathrm{Q}} \tag{11}$$

The cumulative distribution function (CDF) follows from ([18] (8.352.6)):

$$F_{\mathcal{A}_{\mathrm{Q}}}(x) = 1 - \sum_{j_1=0}^{m_{\mathrm{Q}}-1} \cdots \sum_{j_K=0}^{m_{\mathrm{Q}}-1} \sum_{p=0}^{\Delta_{\mathrm{Q}}-1} \frac{\Lambda_{\mathrm{Q}}(K)\Gamma(\Delta_{\mathrm{Q}})}{p!\, \psi_{\mathrm{Q}}^{\Delta_{\mathrm{Q}}-p}\, \delta_{\mathrm{Q}}^{p}} \exp\left(-\frac{\psi_{\mathrm{Q}} x}{\delta_{\mathrm{Q}}}\right) x^{p} \tag{12}$$

3. CONNECTION OUTAGE PERFORMANCE

Let R_{B} and R_{R} be the target rates. The capacity is $\mathcal{C}(\bar{\gamma}_{\mathrm{Q}}) = \log_2(1 + \bar{\gamma}_{\mathrm{Q}})$. The COP is:

$$\begin{aligned} \mathrm{COP} &= 1 - \Pr(\mathcal{C}(\bar{\gamma}_{\mathrm{R}}) > R_{\mathrm{R}},\, \mathcal{C}(\bar{\gamma}_{\mathrm{B}}) > R_{\mathrm{B}}) \\ &= 1 - [1 - F_{\bar{\gamma}_{\mathrm{R}}}(u_{\mathrm{R}})]\,[1 - F_{\bar{\gamma}_{\mathrm{B}}}(u_{\mathrm{B}})] \end{aligned} \tag{13}$$

where $u_{\mathrm{Q}} = 2^{R_{\mathrm{Q}}} - 1$. We need $F_{\bar{\gamma}_{\mathrm{Q}}}(x)$:

Theorem 1 *Under uncorrelated shadowed–Rician fading, the CDF of $\bar{\gamma}_{\mathrm{Q}}$ is:*

$$F_{\bar{\gamma}_{\mathrm{Q}}}(x) = 1 - \sum_{j_1=0}^{m_{\mathrm{Q}}-1} \cdots \sum_{j_K=0}^{m_{\mathrm{Q}}-1} \sum_{p=0}^{\Delta_{\mathrm{Q}}-1} \frac{\Lambda_{\mathrm{Q}}(K)\Gamma(\Delta_{\mathrm{Q}})}{p!\, \psi_{\mathrm{Q}}^{\Delta_{\mathrm{Q}}-p}\, \delta_{\mathrm{Q}}^{p}} \exp\left(-\frac{\psi_{\mathrm{Q}} \varsigma_{\mathrm{Q}} x}{\delta_{\mathrm{Q}}(\varepsilon_{\mathrm{Q}} - x)}\right) \left(\frac{\varsigma_{\mathrm{Q}} x}{\varepsilon_{\mathrm{Q}} - x}\right)^{p} \tag{14}$$

valid for $0 \leq x < \varepsilon_{\mathrm{Q}}$, where $\varepsilon_{\mathrm{Q}} = \nu_{\mathrm{Q}}/(\alpha_{\mathrm{RB}}\beta_{\mathrm{T}})$ for $\mathrm{T} \in \{\mathrm{R}, \mathrm{B}\}$, $\mathrm{T} \neq \mathrm{Q}$, and $\varsigma_{\mathrm{Q}} = \mu_{\mathrm{Q}}/(\alpha_{\mathrm{RB}}\beta_{\mathrm{T}})$

Proof 1 *Use $F_{\bar{\gamma}_{\mathrm{Q}}}(x) = \Pr(\bar{\gamma}_{\mathrm{Q}} < x)$ and (12)*

Substituting (14) into (13) gives the exact COP:

$$\mathrm{COP} = 1 - \prod_{Q \in \{\mathrm{R},\mathrm{B}\}} \left[1 - F_{\bar{\gamma}_{\mathrm{Q}}}(u_{\mathrm{Q}})\right] \tag{15}$$

Diversity order (high SNR). Following the high-SNR asymptotic expansion approach in [20], from (12), for $\varrho_S \to \infty$, a Maclaurin expansion yields ([21], (51)).

$$F_{\mathcal{A}_{\mathrm{Q}}}^{\infty}(x) \simeq \frac{\alpha_{\mathrm{Q}}^{K} x^{K}}{K!\, \delta_{\mathrm{Q}}^{K}} \tag{16}$$

Combining with (15), the asymptotic COP is:

$$\mathrm{COP}^{\infty} = \frac{\alpha_{\mathrm{Q}}^{K}}{K!\, \delta_{\mathrm{Q}}^{K}} \left[\left(\frac{\varsigma_{\mathrm{R}} u_{\mathrm{R}}}{\varepsilon_{\mathrm{R}} - u_{\mathrm{R}}}\right)^{K} + \left(\frac{\varsigma_{\mathrm{B}} u_{\mathrm{B}}}{\varepsilon_{\mathrm{B}} - u_{\mathrm{B}}}\right)^{K}\right] \tag{17}$$

$$\mathrm{IP} = \sum_{j_1=0}^{m_{\mathrm{B}}-1} \cdots \sum_{j_K=0}^{m_{\mathrm{B}}-1} \sum_{p=0}^{\Delta_{\mathrm{B}}-1} \frac{\Lambda_{\mathrm{B}}(K)\Gamma(\Delta_{\mathrm{B}})}{p!\, \psi_{\mathrm{B}}^{\Delta_{\mathrm{B}}-p}\, \delta_{\mathrm{B}}^{p}} \exp\left(-\frac{\psi_{\mathrm{B}} \varsigma_{\mathrm{B}} u_{\mathrm{B}}}{\delta_{\mathrm{B}}(\varepsilon_{\mathrm{B}} - u_{\mathrm{B}})}\right) \left(\frac{\varsigma_{\mathrm{B}} u_{\mathrm{B}}}{\varepsilon_{\mathrm{B}} - u_{\mathrm{B}}}\right)^{p} \tag{18}$$

Remark 1 *The closed-form COP and IP depend on long-term channel statistics (not instantaneous coefficients), enabling low-cost evaluation and design for integrated satellite–terrestrial networks with perfect-CSI baselines.*

Remark 2 *The framework aligns with practical deployments where satellites offer backhaul and gap-filler aided access for indoor handhelds, supporting streaming and broadband connectivity.*

4. RESULTS AND DISCUSSIONS

This section provides numerical simulations to verify the analytical expressions. Shadowed–Rician parameters for the S–Q link follow [22]: heavy shadowing (HS) $(m_{\rm Q}, b_{\rm Q}, \Omega_{\rm Q}) = (1, 0.063, 0.0007)$ and average shadowing (AS) $(5, 0.251, 0.279)$. Unless otherwise stated [16], parameters are $K \in \{1, 2, 3\}$, $R_{\rm R} =$ 1 bits per channel use (BPCU), $R_{\rm B} = 0.5$ BPCU, $\beta_{\rm B} = 0.7$, $\beta_{\rm R} = 0.3$, $\alpha_{\rm B} = \alpha_{\rm R} = (1-\alpha_{\rm RB})/2$, $f_c = 2$ GHz, $W = 15$ MHz, $T = 300$ K, $c = 3 \times 10^8$ m/s, $d_{SQ} = 35786$ km, $\vartheta_S = 53.45$ dB, $\vartheta_{\rm Q} = 4.8$ dB, $\theta_{\rm Q} = 0.8°$, $\theta_{\rm Q,3dB} = 0.3°$, bandwidth (BW) = 10 $MHz, noisefigure(NF) = 10$ dB, $N_0 = -174$ dBm/Hz. The noise power is $\sigma^2_{\rm Q}[{\rm dBm}] = N_0 + 10\log_{10}({\rm BW}) + {\rm NF}$ [23]. Table 2 summarizes key settings.

Table 2. Simulation parameters

Parameter	Value	Description
K	1, 2, 3	Number of satellite antennas
P_S	$[-10, 30]$ dBm	Satellite transmit power
α_{RB}	0.1, 0.2, 0.3	BP for superposition signal
m_Q	1 (HS), 5 (AS)	Fading severity
β_B	0.7	Power allocation for Bob

Figure 2 shows COP vs. P_S (dBm). Increasing K reduces COP via spatial diversity. PFMA with $\alpha_{\rm RB} \in \{0.1, 0.2, 0.3\}$ consistently outperforms NOMA. At higher P_S (> 10 dBm), COP saturates. Agreement between exact and asymptotic curves validates the analysis. Smaller $\alpha_{\rm RB}$ further improves COP by reducing inter-user interference in the combined SINRs. The observed ≈ 4 dB SNR gain (see Figure 3) translates to $\sim 60\%$ coverage extension or up to 37% power saving via the free-space loss with traceability in [15].

$$L_{SQ} = \left(\frac{4\pi f\, d_{SQ}}{c}\right)^2 \tag{19}$$

Figure 3 presents COP vs. P_S for HS and AS, comparing PFMA and NOMA. Exact (solid) and asymptotic (dashed) curves match closely. PFMA consistently outperforms NOMA, with larger gains under HS. Under HS (m_Q=1, b_Q=0.063, Ω_Q=0.0007), COP increases by up to 20% at low P_S relative to AS (m_Q=5, b_Q=0.251, Ω_Q=0.279). Imperfect CSI (MMSE with estimation errors) further degrades COP: a 10% error-variance rise adds ≈5–10% COP, highlighting PFMA's reliance on accurate CSI and its vulnerability to severe shadowing.

Figure 4 shows COP vs. $\beta_{\rm B}$ for $K \in \{1, 2, 3\}$ and $\alpha_{\rm RB} = 0.4$. Larger K reduces COP for both schemes, with PFMA dominating across all $\beta_{\rm B}$. The curves demonstrate the reliability trade-off as $\beta_{\rm B}$ varies. In Figure 5, IP is plotted vs. P_S for PFMA and NOMA. Varying $\alpha_{\rm RB} \in \{0.1, 0.2, 0.3\}$ shows PFMA achieves lower IP for the same P_S. As P_S increases, IP approaches 1 for all schemes, while smaller $\alpha_{\rm RB}$ benefits low-P_S security. Exact curves validate the analysis. Future research may consider additional practical aspects, e.g., hardware RF impairments such as I/Q imbalance [24], security–reliability trade-off with non-ideal untrusted relaying [25], and simultaneous secure-and-covert transmission under practical assumptions [26].

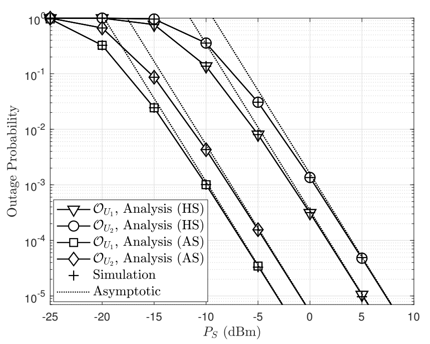

Figure 2. COP comparison: PFMA vs. NOMA

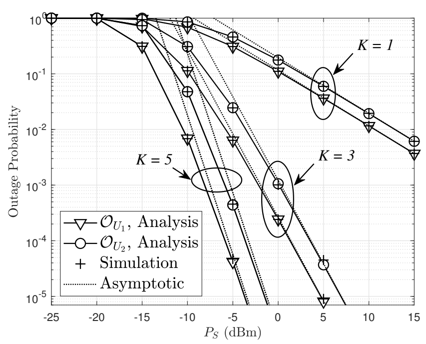

Figure 3. COP vs. P_S under different shadowing; $K = 3$, $\alpha_{\rm RB} = 0.2$

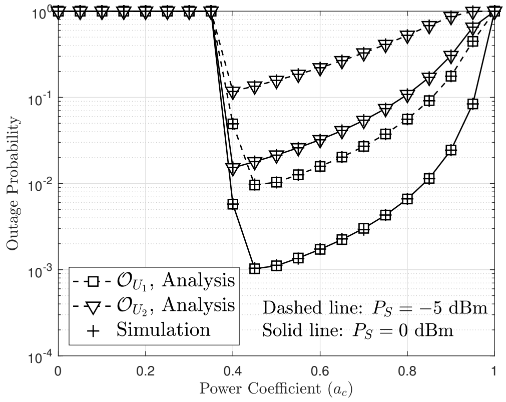

Figure 4. COP vs. β_{B}, $\alpha_{\mathrm{RB}} = 0.4$

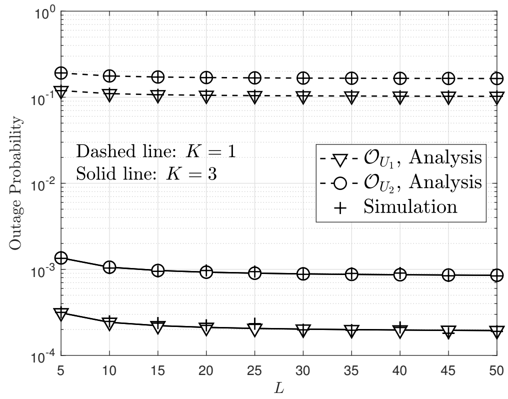

Figure 5. IP vs. P_S (dBm); K=2, R_{R}=R_{B}=1

5. CONCLUSION

We proposed and analyzed a PFMA-based hybrid multiple access framework for secure satellite–terrestrial networks. Closed-form COP and IP expressions (with asymptotics and diversity) under shadowed–Rician fading and dual eavesdroppers reveal ∼4 dB SNR gain over NOMA, up to 30% COP reduction, and 20–25% IP reduction at P_S=10 dBm. Simulations confirm potential ∼60% coverage increase or up to 37% energy saving. Future work will consider multi-cell and mobility scenarios, imperfect self-interference mitigation, optimized BP/PA, multi-antenna transceivers, colluding eavesdroppers, and broader fading models.

ACKNOWLEDGMENT

Authors would like to thank Industrial University of Ho Chi Minh City (IUH) for the support of time and facilities for this study.

FUNDING INFORMATION

This study was self-funded by the authors.

AUTHOR CONTRIBUTIONS STATEMENT

This journal uses the Contributor Roles Taxonomy (CRediT) to recognize individual author contributions, reduce authorship disputes, and facilitate collaboration.

Name of Author	C	M	So	Va	Fo	I	R	D	O	E	Vi	Su	P	Fu
Huu Q. Tran	✓	✓		✓	✓	✓		✓	✓	✓				
Viet-Thanh Pham		✓				✓		✓		✓				

C : **C**onceptualization
M : **M**ethodology
So : **So**ftware
Va : **Va**lidation
Fo : **Fo**rmal Analysis
I : **I**nvestigation
R : **R**esources
D : **D**ata Curation
O : Writing - **O**riginal Draft
E : Writing - Review & **E**diting
Vi : **Vi**sualization
Su : **Su**pervision
P : **P**roject Administration
Fu : **Fu**nding Acquisition

CONFLICTS OF INTEREST

Authors state no conflict of interest.

DATA AVAILABILITY

No new data were generated or analyzed.

REFERENCES

[1] Y. Gu *et al.*, "ISAC towards 6G Satellite–Terrestrial Communications: Principles, Status, and Prospects," *Electronics*, vol. 13, no. 7, p. 1369, 2024, doi: 10.3390/electronics13071369.
[2] S. B. R. Tirmizi, Y. Chen, S. Lakshminarayana, W. Feng, and A. A. Khuwaja, "Hybrid Satellite–Terrestrial Networks toward 6G: Key Technologies and Open Issues," *Sensors*, vol. 22, no. 21, p. 8544, 2022, doi: 10.3390/s22218544.
[3] R. Xu, X. Da, H. Hu, L. Ni, and Y. Pan, "A Secure Hybrid Satellite-Terrestrial Communication Network With AF/DF and Relay Selection," *IEEE Access*, vol. 7, pp. 171980–171994, 2019, doi: 10.1109/ACCESS.2019.2955541.
[4] D. T. Do, A. T. Le, R. Kharel, A. Silva, and M. A. Shattal, "Hybrid Satellite-Terrestrial Relay Network: Proposed Model and Application of Power Splitting Multiple Access," *Sensors*, vol. 20, no. 15, p. 4296, 2020, doi: 10.3390/s20154296.
[5] Q. Ngo, T. K. Phan, A. Mahmood, W. Xiang, "Hybrid IRS-Assisted Secure Satellite-Terrestrial Communications: A Fast Deep Reinforcement Learning Approach," *Institute of Electrical and Electronics Engineers (IEEE)*, Aug. 2022, doi: 10.36227/techrxiv.20478438.v1.
[6] H. Li, *et al.*, "Capacity Upper Bound Analysis of the Hybrid Satellite Terrestrial Communication Systems," *IEEE Commun. Lett.*, vol. 20, no. 12, pp. 2402–2405, 2016, doi: 10.1109/LCOMM.2016.2604387.
[7] H. Li *et al.*, "Performance analysis of the return link for the hybrid satellite terrestrial communication systems," *2016 IEEE 13th International Conference on Signal Processing (ICSP)*, 2016, pp. 1283-1287, doi: 10.1109/ICSP.2016.7878033.
[8] K. An *et al.*, "Performance Analysis of Multi-Antenna Hybrid Satellite-Terrestrial Relay Networks in the Presence of Interference," in *IEEE Transactions on Communications*, vol. 63, no. 11, pp. 4390-4404, Nov. 2015, doi: 10.1109/TCOMM.2015.2474865.
[9] X. Zhang, D. Guo, K. An, G. Zheng, S. Chatzinotas and B. Zhang, "Auction-Based Multichannel Cooperative Spectrum Sharing in Hybrid Satellite-Terrestrial IoT Networks," in *IEEE Internet of Things Journal*, vol. 8, no. 8, pp. 7009-7023, 2021, doi: 10.1109/JIOT.2020.3037408.
[10] P. Ivaniš, J. Milojković, V. Blagojević, and S. Brkić, "Capacity Analysis of Hybrid Satellite–Terrestrial Systems with Selection Relaying," *Entropy*, vol. 26, no. 5, p. 419, 2024, doi: 10.3390/e26050419.
[11] K. Cao *et al.*, "Secure Transmission Designs for NOMA Systems Against Internal and External Eavesdropping," *IEEE Transactions on Information Forensics and Security*, vol. 15, pp. 2930–2943, 2020, doi: 10.1109/TIFS.2020.2980202.
[12] K. S. Ali, A. Al-Dweik, E. Hossain and M. Chafii, "Physical Layer Security of Partial-NOMA and NOMA in Poisson Networks," in *IEEE Transactions on Wireless Communications*, vol. 23, no. 6, pp. 6562-6579, June 2024, doi: 10.1109/TWC.2023.3334020.
[13] C.-B. Le, D.-T. Do, and M. Voznak, "Secure transmission in backhaul NOMA systems: A physical layer security design with untrusted user and eavesdropper," *Digital Communications and Networks*, vol. 10, no. 4, pp. 1001–1013, 2024, doi: 10.1016/j.dcan.2022.12.005.
[14] B. Zhuo *et al.*, "Partial-NOMA Based Physical Layer Security: Forwarding Design and Secrecy Analysis," in *IEEE Transactions on Intelligent Transportation Systems*, vol. 24, no. 7, pp. 7471-7484, 2023, doi: 10.1109/TITS.2022.3166837.
[15] Q. Li, D. Xu, K. Navaie and Z. Ding, "Covert and Secure Communications in NOMA Networks With Internal Eavesdropping," in *IEEE Wireless Communications Letters*, vol. 12, no. 12, pp. 2178-2182, 2023, doi: 10.1109/LWC.2023.3312689.
[16] P. K. Sharma, D. Deepthi, and D. I. Kim, "Outage probability of 3-D mobile UAV relaying for hybrid satellite-terrestrial networks," *IEEE Communications Letters*, vol. 24, no. 2, pp. 418–422, 2020, doi: 10.1109/LCOMM.2019.2956526.
[17] M. W. Akhtar, A. Mahmood, and M. Gidlund, "Partial NOMA for semi-integrated sensing and communication," in *2023 IEEE Globecom Workshops (GC Wkshps)*, 2023, pp. 1129-1134, doi: 10.1109/GCWkshps58843.2023.10464754.
[18] I. S. Gradshteyn, I. M. Ryzhik, A. Jeffrey, Y. V. Geronimus, M. Y. Tseytlin, and Y. C. Fung, "Table of Integrals, Series, and Products," *Journal of Biomechanical Engineering*, vol. 103, no. 1, pp. 58–58, 1981, doi: 10.1115/1.3138251.
[19] V. Bankey, P. K. Upadhyay, D. B. Da Costa, P. S. Bithas, A. G. Kanatas, and U. S. Dias, "Performance Analysis of Multi-Antenna Multiuser Hybrid Satellite-Terrestrial Relay Systems for Mobile Services Delivery," *IEEE Access*, vol. 6, pp. 24729–24745, 2018, doi: 10.1109/ACCESS.2018.2830801.
[20] C.-B. Le, *et al.*, "Joint design of improved spectrum and energy efficiency with backscatter NOMA for IoT," *IEEE Access*, vol. 10, pp. 7504–7519, 2022, doi: 10.1109/ACCESS.2021.3139118.
[21] K. Guo *et al.*, "Power Allocation and Performance Evaluation for NOMA-Aided Integrated Satellite-HAP-Terrestrial Networks Under Practical Limitations," in *IEEE Internet of Things Journal*, vol. 11, no. 7, pp. 13002-13017, 2024, doi: 10.1109/JIOT.2023.3337124.
[22] N. I. Miridakis, D. D. Vergados, and A. Michalas, "Dual-hop communication over a satellite relay and shadowed Rician channels," in *IEEE Transactions on Vehicular Technology*, vol. 64, no. 9, pp. 4031-4040, Sept. 2015, doi: 10.1109/TVT.2014.2361832.
[23] H. Q. Tran and B. M. Lee, "RIS-NOMA-assisted short-packet communication with direct links," *Journal of King Saud University - Computer and Information Sciences*, vol. 36, no. 3, p. 101979, 2024, doi: 10.1016/j.jksuci.2024.101979.
[24] X. Li, M. Zhao, Y. Liu, L. Li, Z. Ding, and A. Nallanathan, "Secrecy analysis of ambient backscatter NOMA systems under I/Q imbalance," *IEEE Transactions on Vehicular Technology*, vol. 69, no. 10, pp. 12286–12290, 2020, doi: 10.1109/TVT.2020.3006478.
[25] A. Kuhestani, A. Mohammadi, and P. L. Yeoh, "Security-reliability trade-off in cyber-physical cooperative systems with non-ideal untrusted relaying," in *2018 IEEE 4th World Forum on Internet of Things (WF-IoT)*, 2018, pp. 552–557, doi: 10.1109/WF-IoT.2018.8355190.
[26] M. Forouzesh, F. S. Khodadad, P. Azmi, A. Kuhestani, and H. Ahmadi, "Simultaneous Secure and Covert Transmissions Against Two Attacks Under Practical Assumptions," *IEEE Internet Things Journal*, vol. 10, no. 12, pp. 10160–10171, 2023, doi: 10.1109/JIOT.2023.3237640.

BIOGRAPHIES OF AUTHORS

Huu Q. Tran (Member, IEEE) received the M.S. degree in Electronics Engineering from Ho Chi Minh City University of Technology and Education (HCMUTE), Vietnam in 2010. Currently, he has been working as a lecturer at Faculty of Electronics Technology, Industrial University of Ho Chi Minh City (IUH), Vietnam. He obtained his Doctorate from the Faculty of Electrical and Electronics Engineering at HCMUTE, Vietnam. His research interests include wireless communications, non-orthogonal multiple access (NOMA), energy harvesting (EH), wireless cooperative relaying networks, heterogeneous networks (HetNet), cloud radio access networks (C-RAN), unmanned aerial vehicles (UAV), reconfigurable intelligent surfaces (RIS), short-packet communication (SPC) and internet of things (IoT). He can be contacted at email: tranquyhuu@iuh.edu.vn.

Viet-Thanh Pham received the Ph.D. degree in Electronics, Automation, and Control of Complex Systems from the University of Catania. He is with the Industrial University of Ho Chi Minh City. His research interests include chaos, nonlinear control, fractional-order systems, mathematical modelling, and applications of nonlinear systems. He can be contacted at email: phamvietthanh@iuh.edu.vn.